Acta Pharmaceutica Sinica B 2025;15(2):1023−1038

Chinese Pharmaceutical Association
Institute of Materia Medica, Chinese Academy of Medical Sciences

Acta Pharmaceutica Sinica B

www.elsevier.com/locate/apsb
www.sciencedirect.com

ORIGINAL ARTICLE

GLP-1RAs attenuated obesity and reversed leptin resistance partly *via* activating the microbiome-derived inosine/A2A pathway

Chunyan Dong, Bailing Zhou, Binyan Zhao, Ke Lin, Yaomei Tian, Rui Zhang, Daoyuan Xie, Siwen Wu, Li Yang*

State Key Laboratory of Biotherapy and Cancer Center, West China Hospital, Sichuan University and Collaborative Innovation Center of Biotherapy, Chengdu 610041, China

Received 4 April 2024; received in revised form 26 June 2024; accepted 24 July 2024

KEY WORDS

Obesity;
GLP-1RAs;
Gut microbiota;
Metabolite;
Obesity-related inflammation;
Leptin resistance;
Macrophage-adipocyte;
A2A pathway

Abstract Extensive evidence has demonstrated that glucagon-like peptide-1 receptor agonists (GLP-1RAs) can ameliorate obesity. Our previous studies revealed that $(Ex\text{-}4)_2$-Fc, a long-acting GLP-1RA we developed, depends on the leptin pathway to treat obesity. However, the mechanisms linking $(Ex\text{-}4)_2$-Fc and leptin resistance remain largely unclear. To address this question, we explored the mechanism of GLP-1RAs from the perspective of the gut microbiota, as increasing evidence indicates an important link between the gut microbiota and obesity. This study aimed to explore the potential role of the gut microbiota in the treatment of GLP-1RAs. We found that $(Ex\text{-}4)_2$-Fc treatment reshaped obesity-induced gut microbiota disturbances and substantially increased the abundance of *Akkermansia muciniphila* (*Am*). In addition, $(Ex\text{-}4)_2$-Fc did not respond well in antibiotic-treated (ATB) Obese mice. Subsequent studies have shown that this defect can be overcome by gavage with *Am*. In addition, we found that *Am* enhanced $(Ex\text{-}4)_2$-Fc therapy by producing the metabolite inosine. Inosine regulates the macrophage adenosine A2A receptor (A2A) pathway to indirectly reduce leptin levels in adipocytes Thus, elucidating the role of metabolites in regulating the leptin pathway will provide new insights into GLP-1RAs therapy and may lead to more effective strategies for guiding the clinical use of antidiabetic agents.

*Corresponding author.
E-mail address: yl.tracy73@gmail.com (Li Yang).

Peer review under the responsibility of Chinese Pharmaceutical Association and Institute of Materia Medica, Chinese Academy of Medical Sciences.

https://doi.org/10.1016/j.apsb.2024.12.006

1. Introduction

Obesity has become a public health problem of great concern in the past few decades. According to the latest updated records from the World Health Organization (WHO), approximately 40% of people worldwide are overweight, whereas 13% are obese[1]. Improving one's lifestyle, adjusting one's eating habits, and increasing one's physical exercise help to treat obesity. However, these approaches do not completely solve the problem of obesity, so some research has focused on treating obesity with drugs[2-4]. Glucagon-like peptide-1 (GLP-1) is a 30-amino acid incretin hormone secreted mainly by L-cells in the distal portion[5]. GLP-1 can control body weight and enhance glucose sensitivity, but endogenous GLP-1 is easily degraded by dipeptidyl peptidase IV (DPP-IV), which has a half-life of 1−2 min, thus limiting the clinical therapeutic potential of natural GLP-1[6,7]. Exendin-4 (Ex-4) is a 39-amino acid peptide isolated from the salivary glands of the Gila monster lizard (*Heloderma suspectum*) that shares 53% sequence homology with GLP-1. Unlike GLP-1, Ex-4 is a stable peptide because it is not easily degraded by DPP-IV[8]. Although Ex-4 has a longer half-life than natural GLP-1, it still needs to be injected once or twice a day[9]. In our previous study, we designed a long-acting GLP-1RA, Exendin-4-IgG4 Fc fusion protein ($(Ex\text{-}4)_2$-Fc), which is essentially two tandem copies of the Ex-4 molecule fused onto a mutated human IgG4 constant heavy chain[10,11]. The half-life of $(Ex\text{-}4)_2$-Fc was significantly extended to 122 h in male Sprague−Dawley (SD) rats[10]. For decades, GLP-1 analogs and their long-acting formulations have been continuously developed and are as effective as GLP-1. For example, from exenatide twice daily (the first approved GLP-1RA) to liraglutide once a day, to albiglutide, dulaglutide, and semeglutide once a week, and even the oral GLP-1RA (semeglutide) approved in 2019. In addition to diabetes, Novo Nordisk's semeglutide injection, Wegovy, has shown promising results in the clinic and was approved by the FDA for the treatment of obesity in 2021[12-16], and extensive evidence has demonstrated that GLP-1RAs can effectively treat obesity[17-20]. Similarly, we found that $(Ex\text{-}4)_2$-Fc can also achieve good weight loss, and this is partly achieved by reducing the leptin levels[10], and Zhao et al.[21] also demonstrated that partial leptin reduction can effectively ameliorate obesity. However, the underlying mechanism by which $(Ex\text{-}4)_2$-Fc reduces leptin to improve obesity remains unclear.

In recent years, the gut microbiota is associated with several diseases, such as obesity, type 2 diabetes (T2D), and alcoholic liver injury[22-25]. It has been observed in clinical practice that not all T2D patients reach therapeutic targets in response to GLP-1-based therapies because their HbA1c is lower than 6.5%, indicating a state of GLP-1 resistance[26,27]. Grasset et al.[28] reported that a specific set of bacteria impaired the GLP-1-activated gut−brain axis to control insulin secretion and gastric emptying and that gut microbiota dysbiosis induced GLP-1 resistance through the gut−brain axis mechanism in animal models. Some studies have shown that obesity induces greater abundances of *Firmicutes*, *Fusobacteria*, *Proteobacteria*, and *Actinobacteria* and a lower abundance of *Bacteroidete*[29-31]. Remarkably, there is also evidence demonstrating the interactions between antidiabetic drugs and the gut microbiota, and drugs could affect host function by altering the gut microbiome and its metabolites (drug−microbial−metabolic axis)[32]. Several studies have highlighted the key role of the gut microbiota in drug therapy, such as the immune checkpoint inhibitors CTLA-4, PD-1, and PD-L1[31,33-37]. Therefore, regulating the gut microbiota composition by drug therapy may be a potential way to treat obesity. Currently, although studies have reported changes in the gut microbiota composition after GLP-1RA treatment, whether the gut microbiota influences its therapeutic efficacy and the related molecular mechanisms remain unclear. The development of GLP-1RAs and next-generation GLP-1 therapies requires a more precise understanding of the mechanisms of action and greater insight into the control of GLP-1R signaling. Our previous research revealed that $(Ex\text{-}4)_2$-Fc can treat obesity by partially lowering leptin[10], and Zhao et al.[21] also demonstrated that partial leptin reduction can effectively ameliorate obesity. However, the underlying mechanism by which $(Ex\text{-}4)_2$-Fc reduces leptin to improve obesity remains unclear.

In our study, we first found that $(Ex\text{-}4)_2$-Fc treatment altered the microbiota and its driven metabolite inosine. In addition, inosine reduced adipocyte leptin levels by regulating adipocyte macrophage A2A signaling, ultimately reversing obesity-induced hypothalamic leptin resistance and improving obesity. Finally, we demonstrated that $(Ex\text{-}4)_2$-Fc plays a therapeutic role through A2A signaling. Taken together, our findings revealed that $(Ex\text{-}4)_2$-Fc reversed obesity-induced hypothalamic leptin antagonism *via* microbiome-derived inosine.

2. Materials and methods

2.1. Chemicals and reagents

High fat diet (HFD) was purchased from Research Diets, Inc. (New Brunswick, USA). Ampicillin, RIPA lysis buffer, protease inhibitors, phosphatase inhibitors, and loading buffer were purchased from Beijing Solarbio Biotechnology Co., Ltd. (Beijing, China). Streptomycin and colistin were obtained from Dalian Meilun Biotechnology Co., Ltd. (Dalian, China). Tryptic Soy Agar (TSA) blood plates and brain heart infusion broth were purchased from Elite Media, Inc. (London, UK). Inosine, isobutylmethylxanthine (IBMX), dexamethasone (DEX), insulin (INS), and ZM241385 were purchased from MedChemexpress (MCE) Biotechnology Co., Ltd. (Monmouth Junction, NJ, USA). Stool DNA isolation kit and RNA isolation kit were purchased from Chengdu Foregene Biotechnology Co., Ltd. (Chengdu, China). The AxyPrep DNA Gel Extraction Kit was purchased from Corning Inc. (Silicon Valley, CA, USA). ChamQ Universal SYBR qPCR Master Mix kit Nanjing Vazyme Biotechnology Co., Ltd. (Nanjing, China). Taq DNA Polymerase Kit was purchased from Takara Holdings Inc. (Dalian, China). The A2A, F4/80, P65, and p-P65 antibodies were purchased from Santa Cruz Biotechnology, Inc. (Dallas, TX, USA). The JNK, p-JNK, P38, p-P38, ERK, p-ERK, and GAPDH antibodies were purchased from Hangzhou HuaAn Biotechnology (Hangzhou, China). The p-STAT3 antibody was purchased from Cell Signaling Technology (CST), Inc. (Boston, MA, USA). Leptin enzyme-linked immunosorbent assay (ELISA) kit was purchased from Bio-Techne (Minneapolis, MN, USA). The insulin ELISA kit was purchased from Merck Millipore (Darmstadt, Germany). Recombinant murine macrophage colony stimulating factor (M-CSF) was purchased from Beijing PrimeGene Science and Technology Co., Ltd. (Beijing, China). Lipopolysaccharide (LPS) was purchased from Beyotime Biotech Inc. (Shanghai, China). Type I collagenase was purchased from Absin Bioscience Inc. (Shanghai, China).

2.2. Animals

Male C57BL/6J mice aged 6−8 weeks were purchased from Beijing Wei Tong Li Hua Biological Technology Co., Ltd. (Beijing, China). The *db/db* and *ob/ob* mice (male, 8 weeks old) were purchased from Hua Fu Kang Biological Technology Co., Ltd. (Sichuan, China). $A2A^{-/-}$ mice were purchased from the Model Animal Research Center (MARC) of Nanjing University (Nanjing, China). $A2A^{-/-}$ mice bred on the C57BL/6J genetic background and their wild-type mice were maintained at the School of Sichuan University (Chengdu, China). All animal experiments were conducted following the guidelines approved by the Ethics Committee of Sichuan University (20190923028).

2.3. Animal studies

2.3.1. $(Ex\text{-}4)_2$-Fc treatment

Male C57BL/6J mice were fed a high-fat diet containing 60% caloric fat (Research Diets, USA) to induce DIO model mice (HFD group), while the mice in the normal group (NC) were fed normal chow. DIO model mice were divided into HFD and $(Ex\text{-}4)_2$-Fc groups. The $(Ex\text{-}4)_2$-Fc group mice were injected with $(Ex\text{-}4)_2$-Fc (1.8 mg/kg, once a week) by subcutaneous injection for 14 days, and the mice were sacrificed after fecal and serum samples were collected. Body weight and food intake were measured during the experiments. WT and $A2A^{-/-}$ mice were fed a high-fat diet to induce obesity. WT mice were divided into the WT and WT+$(Ex\text{-}4)_2$-Fc groups, and $A2A^{-/-}$ mice were divided into the $A2A^{-/-}$ and $A2A^{-/-}$+$(Ex\text{-}4)_2$-Fc groups. The WT+$(Ex\text{-}4)_2$-Fc and $A2A^{-/-}$+$(Ex\text{-}4)_2$-Fc group mice were injected with $(Ex\text{-}4)_2$-Fc (1.8 mg/kg, once a week) by subcutaneous injection for 14 days, and the body weight and food intake of the mice were monitored daily.

2.3.2. Antibiotic treatment experiment

DIO model mice were divided into an antibiotic-treated group (ATB) and an untreated group (HFD). The ATB group mice were supplemented with mixed antibiotics (ampicillin 1 mg/mL; streptomycin 5 mg/mL; colistin 1 mg/mL) in sterile drinking water, which was changed twice a week[33]. The untreated group was divided into HFD and $(Ex\text{-}4)_2$-Fc groups and the treated group was divided into ATB and ATB+$(Ex\text{-}4)_2$-Fc groups. Mice in the $(Ex\text{-}4)_2$-Fc and ATB+$(Ex\text{-}4)_2$-Fc groups were subcutaneously injected with $(Ex\text{-}4)_2$-Fc (1.8 mg/kg, once a week) for 14 days. The body weight and food intake of the mice were monitored daily.

2.3.3. Supplemental Am cotherapy

ATB mice were divided into ATB, ATB+$(Ex\text{-}4)_2$-Fc and ATB+$(Ex\text{-}4)_2$-Fc + Am groups, and HFD-fed mice were divided into HFD and $(Ex\text{-}4)_2$-Fc groups. In the ATB+$(Ex\text{-}4)_2$-Fc + Am group, *Am* was administered by oral gavage (10^8 CFU/200 μL, once daily) starting two weeks before $(Ex\text{-}4)_2$-Fc treatment. *Am* (ATCC BAA-835) was purchased from the American Type Culture Collection (ATCC) and cultured at 37 °C in an anaerobic incubator containing 100% nitrogen. *Am* was evenly coated on TSA blood plates (ELITE-MEDIA, UK) and cultured for 24 h. On the second day, *Am* was collected and diluted to the desired concentration using brain heart infusion broth (ELITE-MEDIA, UK). Then, the diluted *Am* suspension was treated by gavage, and part of the suspension was evenly coated on a TSA blood plate for further culture. The body weight and food intake of the mice were monitored daily after the $(Ex\text{-}4)_2$-Fc treatment began.

2.3.4. Supplemental inosine co-therapy

ATB mice were divided into ATB, ATB+$(Ex\text{-}4)_2$-Fc and ATB+$(Ex\text{-}4)_2$-Fc + Inosine groups, and HFD-fed mice were divided into HFD and $(Ex\text{-}4)_2$-Fc groups. The ATB+$(Ex\text{-}4)_2$-Fc + Inosine group mice were given inosine (MCE, USA) by oral gavage (300 mg/kg, once daily) for 14 days from the first day of $(Ex\text{-}4)_2$-Fc treatment[33]. The body weight and food intake of the mice were monitored daily.

2.3.5. Inosine treatment

DIO model mice were divided into HFD and inosine groups. The inosine group was given inosine (300 mg/kg, once daily) for 14 days. The *db/db* mice were divided into *db/db* NS and *db/db* NS + Inosine groups. The *ob/ob* mice were divided into the *ob/ob* NS and *ob/ob* NS + Inosine groups. The *db/db* NS + Inosine group and *ob/ob* NS + Inosine group mice were given inosine (300 mg/kg, once daily) for 14 days. The body weight and food intake of the mice were monitored daily after inosine treatment. Similarly, inosine treatment was administered to WT and A2A obese mice, and the body weight and food intake of the mice were monitored daily.

2.4. Glucose tolerance test

For the glucose tolerance tests (IPGTTs), mice were fasted for 15 h before receiving an intraperitoneal injection of glucose at a dose of 2 g/kg. Blood glucose at different time points (0, 30, 60, and 120 min) was measured with a portable glucometer.

2.5. Fecal microbiome 16S rRNA detection and analysis

Fecal samples were collected after 14 days of $(Ex\text{-}4)_2$-Fc treatment. DNA in the fecal samples was extracted using a Stool DNA isolation kit (Foregene, China) according to the manufacturer's instructions. The variable region 4 (V4) region of the microbial 16S rRNA gene was amplified. PCR products were then extracted from agarose gels and purified using the AxyPrep DNA Gel Extraction Kit (Axygen, USA). Purified amplicons were sequenced using an Illumina HiSeq sequencer and QIIME or R to analyze the gut microbiota diversity at Beijing Novogene Co., Ltd. (Beijing, China).

2.6. Untargeted metabonomics

Serum samples were processed and injected into the LC−MS/MS system according to the methods of the Beijing Novogene Co., Ltd. (Beijing, China). UHPLC−MS/MS analyses were performed using a Vanquish UHPLC system (ThermoFisher, Germany) coupled with an Orbitrap Q Exactive HF mass spectrometer (ThermoFisher, Germany) by Beijing Novogene Co., Ltd. (Beijing, China). Statistical analyses were performed using the statistical software R (R version R-3.4.3), Python (Python 2.7.6 version), and CentOS (CentOS release 6.6).

2.7. High-performance liquid chromatography (HPLC)

The serum sample inosine concentration was determined by HPLC (Agilent, Germany). The mobile phase was methanol and formic acid in water. The stationary phase was a C18 column (250 mm × 4.6 mm, Agilent, Germany), and the column temperature was 25 °C. The flow rate was 1 mL/min.

2.8. PCR analysis

Real-time PCR (RT-PCR) analysis. RNA isolation was performed according to the manufacturer's instructions (Foregene, China). RT-PCR was conducted with a ChamQ Universal SYBR qPCR Master Mix kit (Vazyme, China). The relative expression of genes was normalized to that of *Gapdh*. All of the sequences of primers used for RT-PCR are listed in Supporting Information Table S1.

Genomic DNA isolation and PCR. The tails of the partially propagated mice were subjected to PCR to determine the effect of the gene knockout. The tails were added to a tube filled with 75 μL of liquid A and 1 mL of 1 mol/L NaOH +80 μL of 0.1 mol/L EDTA. After cooling at 4 °C to room temperature, 75 μL of Tris-HCl was added, the mixture was vortexed, oscillated for 5 s, and centrifuged at 12,000 rpm for 5 min. Genomic DNA was extracted from the supernatant for PCR identification using a Taq DNA Polymerase Kit (Takara, China). Based on the design results, a 623 bp target band was obtained from the WT mice by PCR amplification with the P3 and P4 primers, while a 948 bp target band was obtained from the $A2A^{-/-}$ mice by PCR amplification with the P1 and P2 primers.

2.9. Protein extraction and Western blot analysis

Lysates were prepared using RIPA (Solarbio, China) buffer containing protease inhibitors (Solarbio, China) and phosphatase inhibitors (Solarbio, China) on ice and centrifuged at 12,000 × *g* for 10 min at 4 °C, after which the protein in the supernatant was collected. The extracts were added to the loading buffer (Solarbio, China) and denatured by boiling at 100 °C for 10 min. The protein samples were electrophoresed on 10% SDS-PAGE gels and transferred to a PVDF membrane. The membranes were blocked with 5% nonfat milk and then incubated with antibodies against A2A (Santa Cruz, USA), P65 (Santa Cruz, USA), p-P65 (Santa Cruz, USA), JNK (Huabio, China), p-JNK (Huabio, China), P38 (Huabio, China), p-P38 (Huabio, China), ERK (Huabio, China), p-ERK (Huabio, China), and GAPDH (Huabio, China). After incubation with the corresponding secondary antibodies and washing with TBST, images were collected using a chemiluminescence imaging system (Clinx, Shanghai, China).

2.10. Histological analysis

Hematoxylin and eosin (HE) staining of eWAT was performed by Lilai (Chengdu, China). Briefly, the sections were deparaffinized and rehydrated, and the nuclei were stained with hematoxylin for 15 min. The sections were then rinsed in running tap water, stained with eosin for 3 min, dehydrated, and mounted. Images were obtained with BA210Digital (Motic). The size of adipocytes was analyzed in HE-stained sections with ImageJ software. The size of the adipocytes was analyzed by ImageJ software, and the average adipocyte area of each group was analyzed statistically by GraphPad software.

Immunofluorescence (IF) staining of eWAT was performed by Hubei Biossci Co., Ltd. (Wuhan, China). Briefly, the sections were blocked for 30 min at room temperature, incubated with primary antibodies against F4/80 (Santa Cruz, USA) and A2A (Santa Cruz, USA) at 4 °C overnight, and then incubated with secondary Alexa Fluor 488 donkey anti-mouse antibody and Alexa Fluor 594 donkey anti-rabbit antibody at 37 °C for 45 min. Images were obtained with a BX51 microscope (Olympus). For the hypothalamus tissues, the sections were blocked for 1 h at room temperature, incubated with primary antibodies against p-STAT3 (CST, USA) overnight at 4 °C, and then incubated with a secondary goat anti-rabbit IgG H&L (Alexa Fluor 555) antibody for 1 h at room temperature. Images were captured using a Zeiss Axioplan 2 imaging system (Zeiss). The positive cells were statistically analyzed by ImageJ software.

2.11. ELISA analysis

Serum leptin concentrations were determined using mouse ELISA kits (R&D, USA). Serum insulin concentrations were determined using a mouse insulin ELISA kit (Millipore, Germany).

2.12. Cell culture

The preadipocyte cell line 3T3-L1 (ATCC, CL-173) was purchased from ATCC. The cells were cultured in high-glucose Dulbecco's modified Eagle's medium (DMEM) with 10% FBS, 100 U/mL penicillin, and 100 μg/mL streptomycin. 3T3-L1 cells were induced to differentiate into mature adipocytes. Briefly, 2 days after confluence (Day 0), the cells were placed in differentiation medium consisting of DMEM, 10% FBS, 0.5 mmol/L IBMX (MCE, USA), 1 μmol/L DEX (MCE, USA), and 10 μg/mL INS (MCE, USA) and then switched to maintenance medium supplemented with DMEM, 10% FBS and 10 μg/mL INS. The medium was replenished every other day.

BMDMs were isolated from C57BL/6J mice. BMDMs were cultured in 1640 medium with 10% FBS, 100 U/mL penicillin, 100 μg/mL streptomycin, and 20 ng/mL M-CSF (prime gene, China) for one week. For cytokine detection, BMDMs were treated with 100 ng/mL LPS (Beyotime, China), 20 mmol/L inosine (MCE, China) or 1 μmol/L ZM241385 (MCE, China) for 6 h[38]. *In vitro*, BMDMs and 3T3-L1 cells were co-cultured. BMDMs were induced with 100 ng/mL LPS (Beyotime, China), 20 mmol/L inosine (MCE, China) or 1 μmol/L ZM241385 (MCE, China) for 24 h before co-culture with mature 3T3-L1 cells[39]. Leptin expression was detected in the cells after 24 h co-culture.

SVFs were isolated from eWAT. Briefly, eWAT was cut into small pieces and digested with type I collagenase (Absin, China) for 30 min at 37 °C. The digestion was terminated, and red cell lysate was cleaved to dissolve the red cells. The SVFs were cultured in DMEM supplemented with 10% FBS overnight. The next day, the cells were incubated with inosine (20 mmol/L) or ZM241385 (1 μmol/L) at 37 °C for 24 h, after which the expression level of leptin was measured.

2.13. Statistical analysis

Unless otherwise specified, statistical analyses were performed with Student's *t*-test (two groups) and two-way ANOVA (more than two groups), followed by Tukey's multiple comparisons test, where appropriate, using GraphPad Prism software. The data are presented as the mean ± standard error of mean (SEM), and a P value < 0.05 was considered to indicate statistical significance.

3. Results

3.1. $(Ex\text{-}4)_2$-Fc reshaped obesity-induced gut microbiota dysbiosis

Growing evidence indicates that obesity induces gut microbiota dysbiosis. We analyzed the changes in the gut microbiota after

$(Ex\text{-}4)_2$-Fc treatment by 16S rRNA sequencing of fecal samples. The results revealed alterations in alpha (Fig. 1A) and beta diversities (Fig. 1B) after $(Ex\text{-}4)_2$-Fc treatment. At the phylum level, the abundances of *Bacteroidetes* and *Verrucomicrobia* increased, while those of *Firmicutes*, *Actinobacteria*, and *Proteobacteria* decreased significantly after $(Ex\text{-}4)_2$-Fc treatment (Fig. 1C). At the species level, obesity-induced some changes in bacterial abundance, while $(Ex\text{-}4)_2$-Fc treatment reversed these bacteria from returning to normal and increased the abundances of some specific bacteria, especially *Am* (Fig. 1D and E). These findings showed that the gut microbiota composition was reshaped after $(Ex\text{-}4)_2$-Fc treatment.

3.2. *ATB mice showed a diminished response to GLP-1RAs, but gavage of Am overcame this deficiency*

Next, we determined whether the efficacy of $(Ex\text{-}4)_2$-Fc therapy was related to the gut microbiota (Fig. 2A). We determined that antibiotics in the drinking water eliminated bacteria in HFD-fed mice by detecting the fecal genome content (Supporting

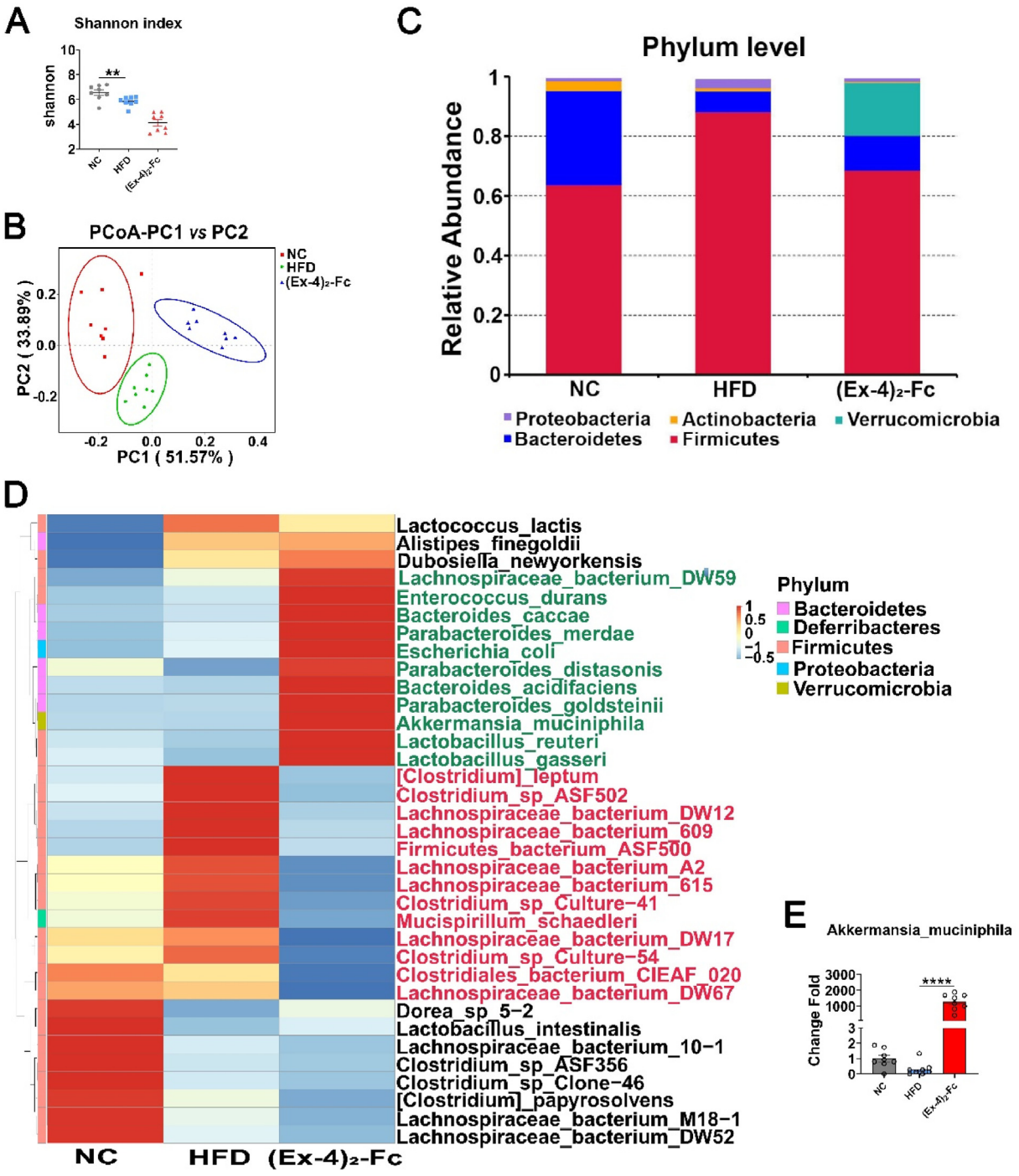

Figure 1 $(Ex\text{-}4)_2$-Fc reshaped obesity-induced gut microbiota dysbiosis. (A) α-Diversity analysis. (B) PCoA analysis. (C, D, E) Microbiome abundance. Data are shown as the mean ± SEM, $^{**}P < 0.01$, $^{****}P < 0.0001$ *versus* the other group, $n = 8$.

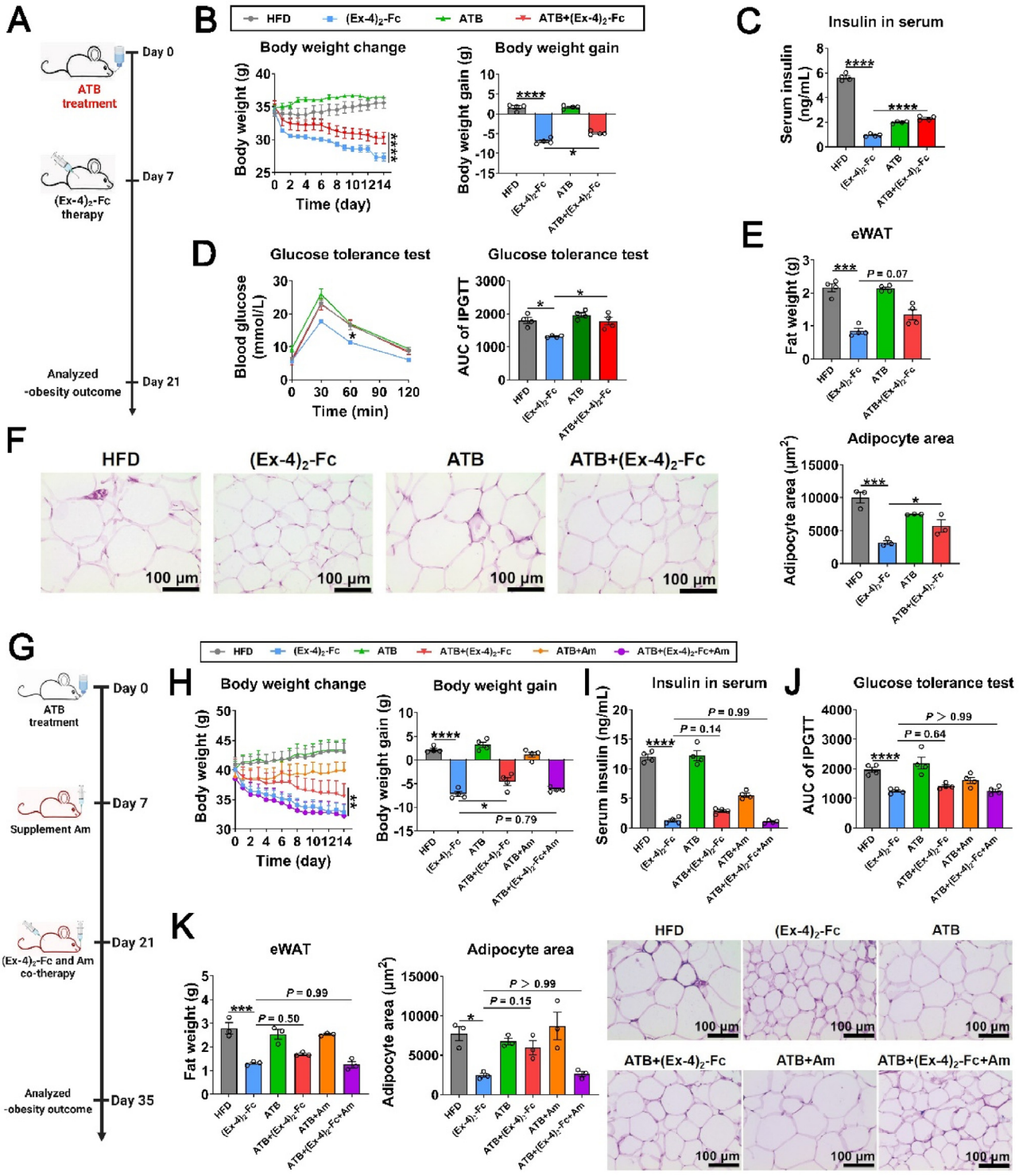

Figure 2 ATB mice showed a diminished response to GLP-1RAs, but gavage of *Am* overcame this deficiency. (A) Experimental schematic. (B) Body weight change ($n = 4$). (C) Insulin concentrations ($n = 4$). (D) Blood glucose levels ($n = 5$). (E) eWAT weight. (F) HE staining results ($n = 3$–4). (G) Experimental schematic. (H) Body weight change ($n = 4$). (I) Insulin concentrations ($n = 4$). (J) Blood glucose levels ($n = 4$). (K) HE staining results and eWAT weight ($n = 3$). The data are shown as the mean ± SEM, $^{ns}P > 0.05$, $^{*}P < 0.05$, $^{**}P < 0.01$, $^{***}P < 0.001$, $^{****}P < 0.0001$ *versus* the other groups.

Information Fig. S1A) and culturing bacteria (Fig. S1B). Compared to the ATB+(Ex-4)$_2$-Fc group, the (Ex-4)$_2$-Fc group showed more significant weight loss and less body weight gain (Fig. 2B). Relatively lower food intake was observed in the (Ex-4)$_2$-Fc group (Fig. S1C). Lower insulin levels were observed in the (Ex-4)$_2$-Fc group than in the other groups, which led to the alleviation of obesity-induced insulin resistance (Fig. 2C). The (Ex-4)$_2$-Fc group had lower glucose levels and areas under the

curve (AUCs) than the other groups according to the IPGTTs (Fig. 2D). HE staining revealed that the adipocyte area in the $(Ex\text{-}4)_2$-Fc group was smaller than that in the ATB+$(Ex\text{-}4)_2$-Fc group (Fig. 2F), and the epididymal adipose tissue (eWAT) weight in the $(Ex\text{-}4)_2$-Fc group was lower (Fig. 2E). The above results indicate that the gut microbiota was closely related to $(Ex\text{-}4)_2$-Fc therapy.

We performed an *Am* and $(Ex\text{-}4)_2$-Fc co-therapy test in ATB mice to validate whether supplementation with *Am* restored $(Ex\text{-}4)_2$-Fc efficacy (Fig. 2G). Interestingly, the ATB+$(Ex\text{-}4)_2$-Fc + Am group and $(Ex\text{-}4)_2$-Fc group had similar therapeutic effects, with more significant weight loss and lower body weight gain than the ATB+$(Ex\text{-}4)_2$-Fc group (Fig. 2H) but no significant change in food intake (Supporting Information Fig. S2A). The insulin levels and glucose tolerance of the ATB+$(Ex\text{-}4)_2$-Fc + Am and $(Ex\text{-}4)_2$-Fc groups were better than those of the ATB+$(Ex\text{-}4)_2$-Fc group (Fig. 2I and J). Additionally, HE staining revealed that the adipocyte areas in the ATB+$(Ex\text{-}4)_2$-Fc + Am and $(Ex\text{-}4)_2$-Fc groups were smaller than those in the ATB+$(Ex\text{-}4)_2$-Fc group, and the eWAT weights in the ATB+$(Ex\text{-}4)_2$-Fc group were significantly greater than those in the ATB+$(Ex\text{-}4)_2$-Fc + Am and $(Ex\text{-}4)_2$-Fc groups (Fig. 2K). These results suggested that supplementation with *Am* restored the side effects of $(Ex\text{-}4)_2$-Fc therapy on the gut microbiota.

3.3. *Microbiota-driven inosine enhanced the efficacy of $(Ex\text{-}4)_2$-Fc in ATB mice*

To understand the mechanism by which the gut microbiota affects $(Ex\text{-}4)_2$-Fc efficacy, we analyzed serum metabolism by untargeted metabolomics (Fig. 3A). The PCA ordination plot revealed that the overall distribution of metabolites significantly differed after $(Ex\text{-}4)_2$-Fc therapy (Fig. 3B). There were 154 different metabolites after $(Ex\text{-}4)_2$-Fc treatment and the top 3 metabolites were xanthine, hypoxanthine, and inosine (Fig. 3C and D). These three metabolites are products of purine metabolism, and inosine metabolism results in the production of xanthine and hypoxanthine[28]. In addition, the use of HPLC technology also demonstrated that the serum creatinine concentration increased after treatment (Supporting Information Fig. S3). To determine the relationship between the gut microbiota and metabolites, we performed an association analysis between the gut microbiota and metabolites. The results showed that *Am* was positively correlated with inosine (Fig. 3E). Mager et al. proved that inosine was the metabolite produced by *Am*[33]. We also confirmed that the serum inosine concentration increased after *Am* administration (Fig. 3F). The above results indicated that changes in the gut microbiota affected purine metabolism after $(Ex\text{-}4)_2$-Fc treatment. Therefore, we speculated that the gut microbiota might impact $(Ex\text{-}4)_2$-Fc therapy *via* the metabolite inosine.

We performed the inosine and $(Ex\text{-}4)_2$-Fc co-therapy test in ATB mice (Fig. 3G). Excitingly, inosine and $(Ex\text{-}4)_2$-Fc co-therapy also enhanced the effect of $(Ex\text{-}4)_2$-Fc in ATB mice. The ATB+$(Ex\text{-}4)_2$-Fc + Inosine and $(Ex\text{-}4)_2$-Fc groups had similar therapeutic effects, with more significant weight loss and lower body weight gain than the ATB+$(Ex\text{-}4)_2$-Fc group (Fig. 3H), but no significant change in food intake (Fig. S2B). Insulin levels, glucose tolerance, and fat-related indicators in the ATB+$(Ex\text{-}4)_2$-Fc + Inosine and $(Ex\text{-}4)_2$-Fc groups were greater than those in the ATB+$(Ex\text{-}4)_2$-Fc group (Fig. 3I−K). These results suggest that supplementation with inosine enhanced $(Ex\text{-}4)_2$-Fc efficacy in ATB mice.

3.4. *Inosine reversed obesity-induced hypothalamic leptin resistance and improved obesity*

Based on the above studies, we hypothesized that $(Ex\text{-}4)_2$-Fc reversed obesity-induced hypothalamic leptin resistance through the metabolite inosine. We therefore designed experiments to verify whether inosine can treat obesity and reverse obesity-induced leptin resistance (Fig. 4A). Lower body weights and body weight gain were observed in the inosine-treated group (Fig. 4B). Inosine treatment effectively reduced food intake (Fig. S2C). Insulin (Fig. 4C) and glucose levels (Fig. 4D) were lower in the NC and inosine groups than in the HFD group. HE staining revealed that the adipocyte area and eWAT weight in the NC and inosine groups were smaller than those in the HFD group (Fig. 4E).

Further studies revealed lower circulating leptin and eWAT leptin expression levels in the inosine group (Fig. 4F). Leptin acts on the hypothalamus to decrease food intake and increase energy expenditure, requiring signal transducer and activator of transcription 3 (STAT3) signaling[23]. We also found that inosine-treated mice had increased phosphorylated STAT3 (p-STAT3) protein expression and p-$STAT3^+$ cell numbers in the hypothalamus (Fig. 4G and H), and supplementation with the STAT3 antagonist S3I-201 partially blocked the therapeutic effects of inosine (Supporting Information Fig. S4). These results support the hypothesis that inosine could improve obesity and reverse obesity-induced leptin resistance (Fig. 4I).

3.5. *Inosine therapy for obesity via the leptin pathway*

Next, we tested whether inosine could cure obesity *via* the leptin pathway using leptin-deficient (*ob*/*ob*) and leptin receptor-deficient (*db*/*db*) mice (Fig. 5A). Body weight, weight gain, and food intake did not differ between *db*/*db* and *ob*/*ob* mice after inosine treatment (Fig. 5B, Fig. S2D). In addition, inosine treatment did not significantly improve the insulin sensitivity, glucose tolerance, or adipose tissue of *db*/*db* or *ob*/*ob* mice (Fig. 5C−F). These results suggest that inosine action depended on the leptin pathway.

3.6. *Inosine inhibited obesity-related inflammation by regulating the macrophage A2A pathway*

We next explored the mechanism by which inosine reduces leptin production in adipocytes. Adenosine catabolism produces inosine, which also plays an anti-inflammatory role through adenosine receptor signaling[24]. Therefore, we examined whether inosine regulated adipocyte leptin secretion by targeting adenosine receptors (Supporting Information Fig. S5A). Transcriptome sequencing analysis of four adenosine receptors, namely, Adaor1 receptor (A1), A2A, Adaor2b receptor (A2B), and Adaor3 receptor (A3), in eWAT, after $(Ex\text{-}4)_2$-Fc treatment revealed that only A2A expression increased (Fig. S5B). Thus, we speculated that inosine may regulate adipocyte leptin secretion by activating A2A. Western blot and RT-PCR analyses also revealed the inosine-activated A2A expression in eWAT (Fig. 6A). Immunofluorescence analysis revealed that A2A was co-expressed with macrophage marker F4/80, but not with adipocytes (Fig. 6B). The number of $F4/80^+$+$A2A^+$ cells in the inosine group was greater than that in the HFD group (Fig. 6B and C). This result indicated that inosine mainly activated A2A in eWAT macrophages. Using *in vitro* simulated cell models, we also demonstrated that inosine

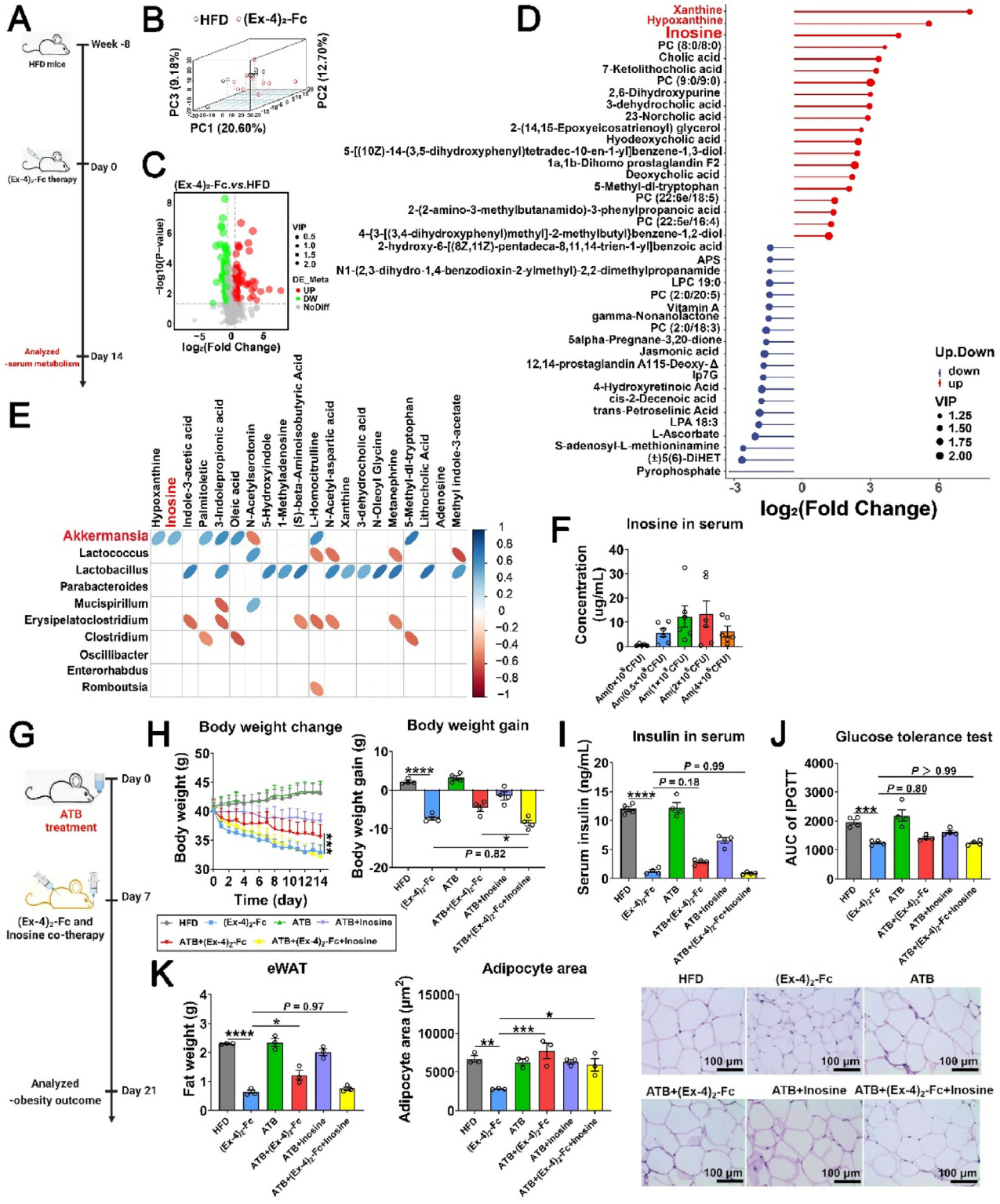

Figure 3 Microbiota-driven inosine enhanced the efficacy of $(Ex\text{-}4)_2$-Fc in ATB mice. (A) Experimental schematic. (B) Metabolite distribution ($n = 10$). (C, D) Metabolites ($n = 10$). (E) Correlation analysis ($n = 10$). (F) Inosine concentration ($n = 6$). (G) Experimental schematic. (H) Body weight change ($n = 4$). (I) Insulin concentrations ($n = 4$). (J) Blood glucose levels ($n = 4$). (K) HE staining results and eWAT weight ($n = 3$). Data are shown as the mean ± SEM, $^{ns}P > 0.05$, $^{*}P < 0.05$, $^{**}P < 0.01$, $^{***}P < 0.001$, $^{****}P < 0.0001$ *versus* the other groups.

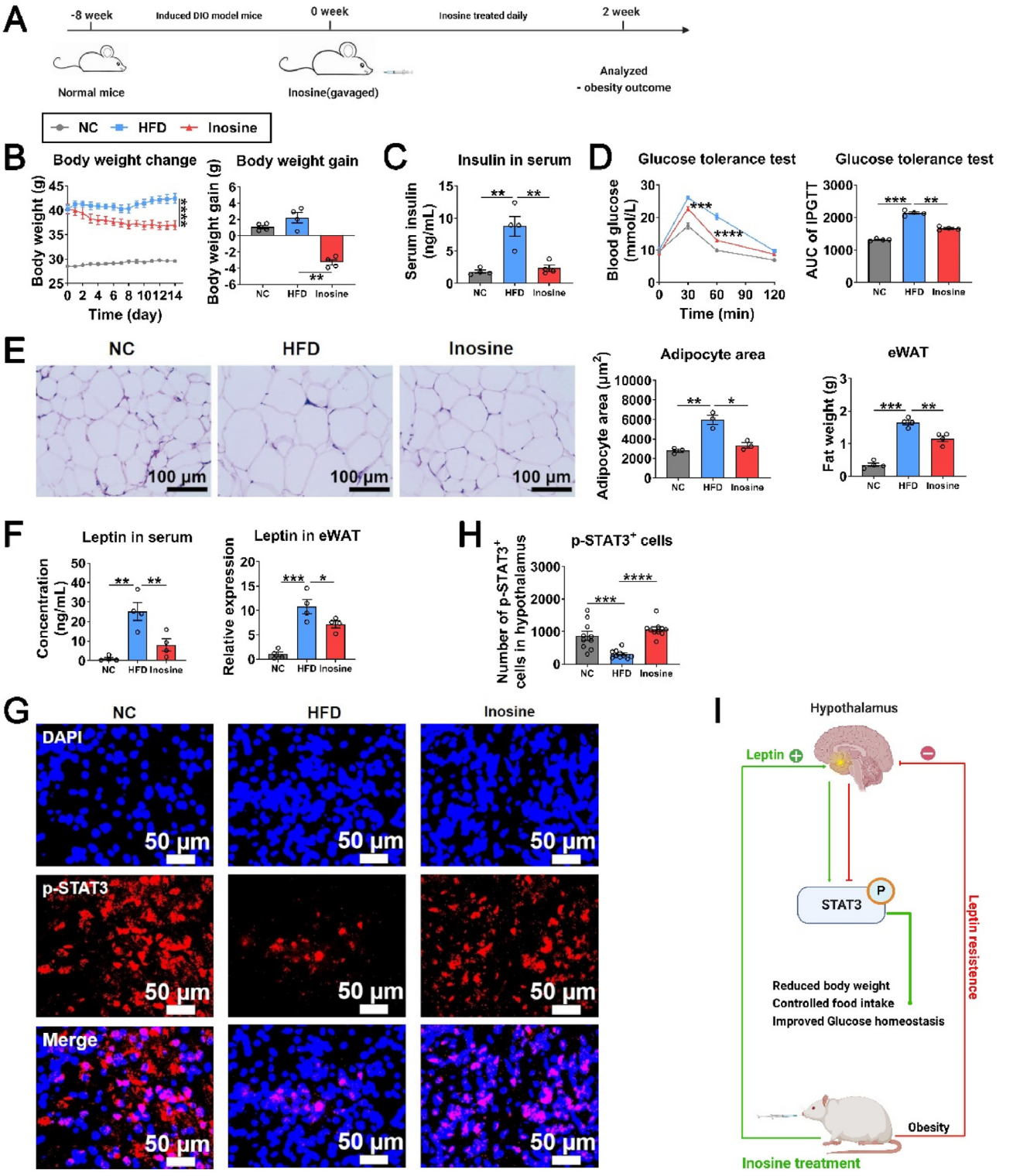

Figure 4 Inosine reversed obesity-induced hypothalamic leptin resistance and improved obesity. (A) Experimental schematic. (B) Body weight change ($n = 4$). (C) Insulin levels ($n = 4$). (D) Blood glucose levels ($n = 4$). (E) HE staining results and eWAT weight ($n = 3-4$). (F) Leptin concentrations and expression levels ($n = 4$). (G, H) Immunofluorescence results and p-STAT3^{+} cells in the hypothalamus. (I) Mechanism of action of inosine. Data are shown as mean ± SEM, $^{*}P < 0.05$, $^{**}P < 0.01$, $^{***}P < 0.001$, $^{****}P < 0.0001$ *versus* the other groups.

activated A2A expression in bone marrow-derived macrophages (BMDMs) but not in 3T3-L1 cells (Fig. S5C).

Obesity induces adipose tissue-related inflammation, such as increased IL-6 and TNF-α expression levels[40]. Previous studies have shown that A2A signaling attenuates LPS-induced macrophage inflammation[39,40]. Our results demonstrate that inosine regulated A2A signaling-related downstream protein expression and the expression of proinflammatory cytokines in eWAT

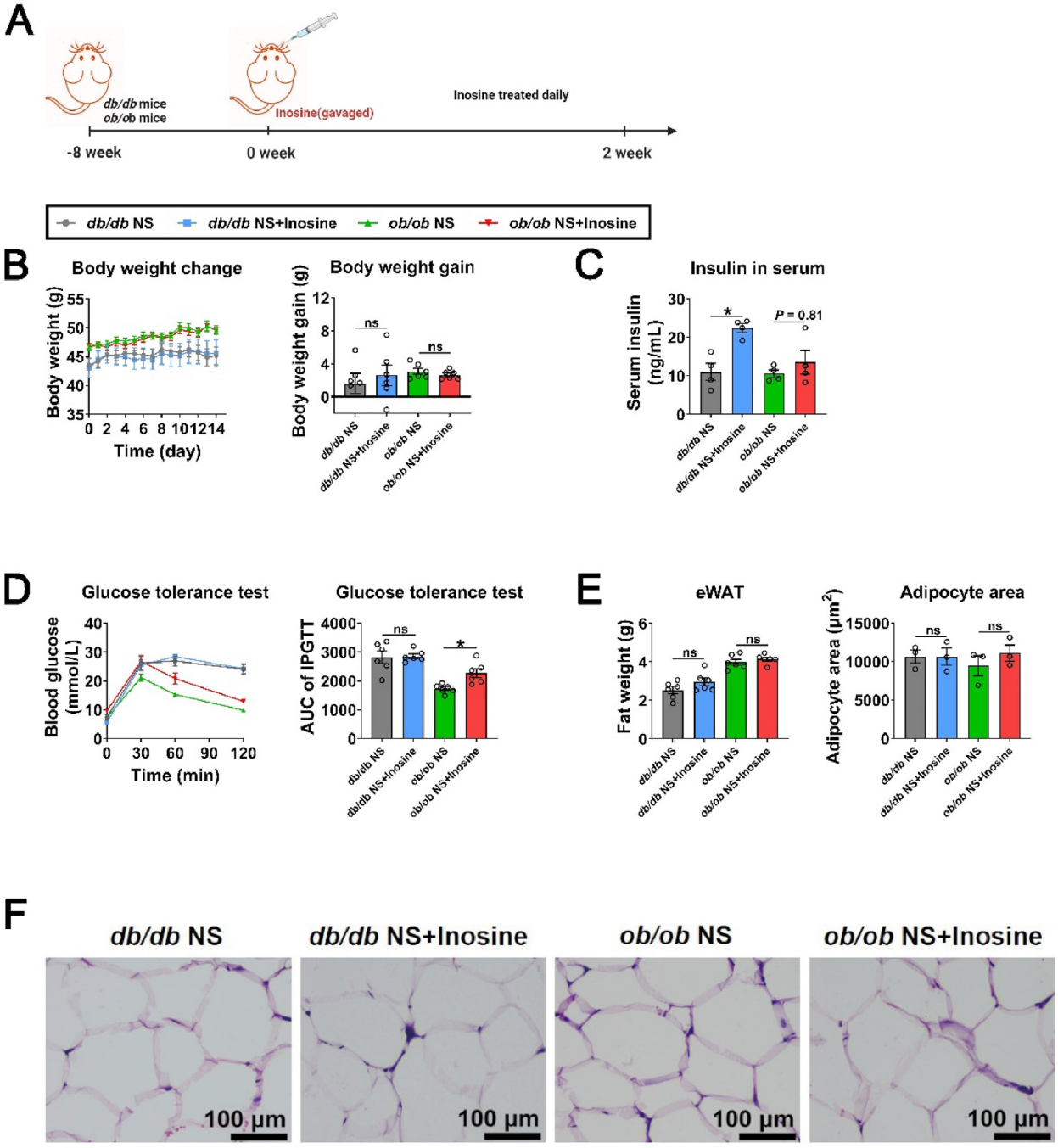

Figure 5 Inosine therapy for obesity *via* the leptin pathway. (A) Experimental schematic. (B) Body weight change ($n = 5$). (C) Insulin concentrations ($n = 4$). (D) Blood glucose levels ($n = 6$). (E, F) HE staining results and eWAT weight ($n = 3-6$). Data are shown as the mean ± SEM, $^{ns}P > 0.05$, $^{*}P < 0.05$ *versus* the other group.

(Fig. 6D, Fig. S5D). Inosine also inhibited proinflammatory cytokine expression in BMDMs, and this effect was partially reversed by treatment with ZM241385 (an A2A antagonist) (Fig. 6E). Moreover, flow cytometry was used to analyze the proportions of M1-type macrophages with pro-inflammatory effects and M2-type macrophages with anti-inflammatory effects in eWAT. The results showed that inosine therapy increased the number of M2-type cells and decreased the number of M1-type cells (Fig. S5E). These results indicate that inosine inhibited obesity-related inflammation by regulating macrophage A2A signaling.

3.7. Inosine indirectly reduced adipocyte leptin levels by regulating macrophages

To better mimic the environment of inosine in eWAT, we isolated and cultured adipose tissue stromal vascular cells (SVFs) from normal and obese mice. The results showed that inosine reduced

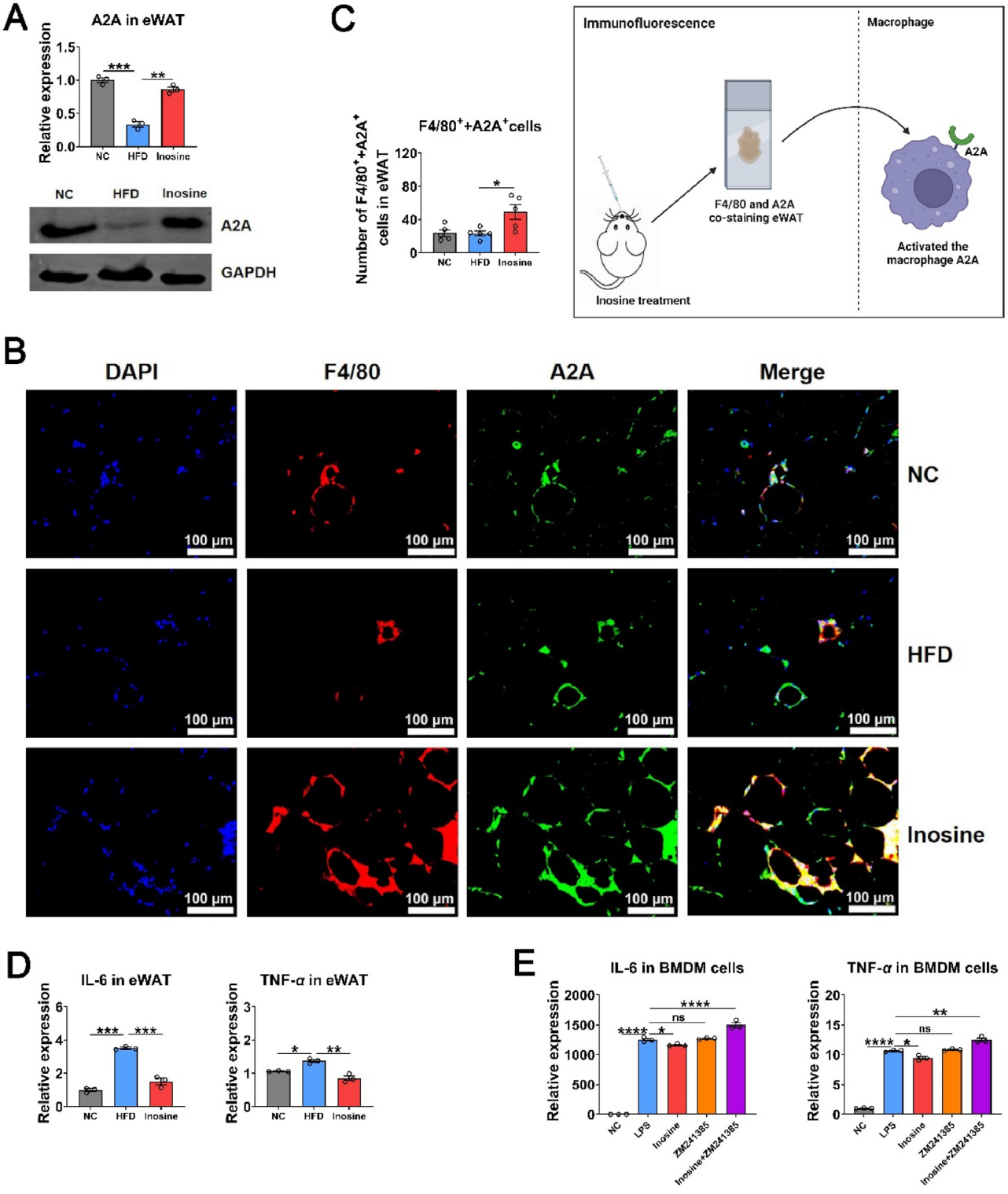

Figure 6 Inosine suppressed obesity-related inflammation in a manner dependent on macrophage A2A activation. (A) A2A expression in eWAT ($n = 3$). (B, C) Immunofluorescence results and F4/80^{+}+A2A^{+} cell numbers ($n = 5$). (D, E) Proinflammatory factor expression in eWAT and BMDMs ($n = 3$). Data are shown as mean ± SEM, $^{ns}P > 0.05$, $^{*}P < 0.05$, $^{**}P < 0.01$, $^{***}P < 0.001$, $^{****}P < 0.0001$ *versus* the other groups.

the expression of leptin, and the ability of inosine to inhibit leptin expression was partially abrogated after treatment with ZM241385 (Fig. 7A). In addition, inosine did not directly inhibit leptin secretion in LPS-stimulated 3T3-L1 cells but increased leptin expression (Fig. 7B). Therefore, we hypothesized that inosine may indirectly reduce adipocyte leptin expression by inhibiting macrophage inflammation. We tested our hypothesis by performing validation experiments, coculturing inosine-treated

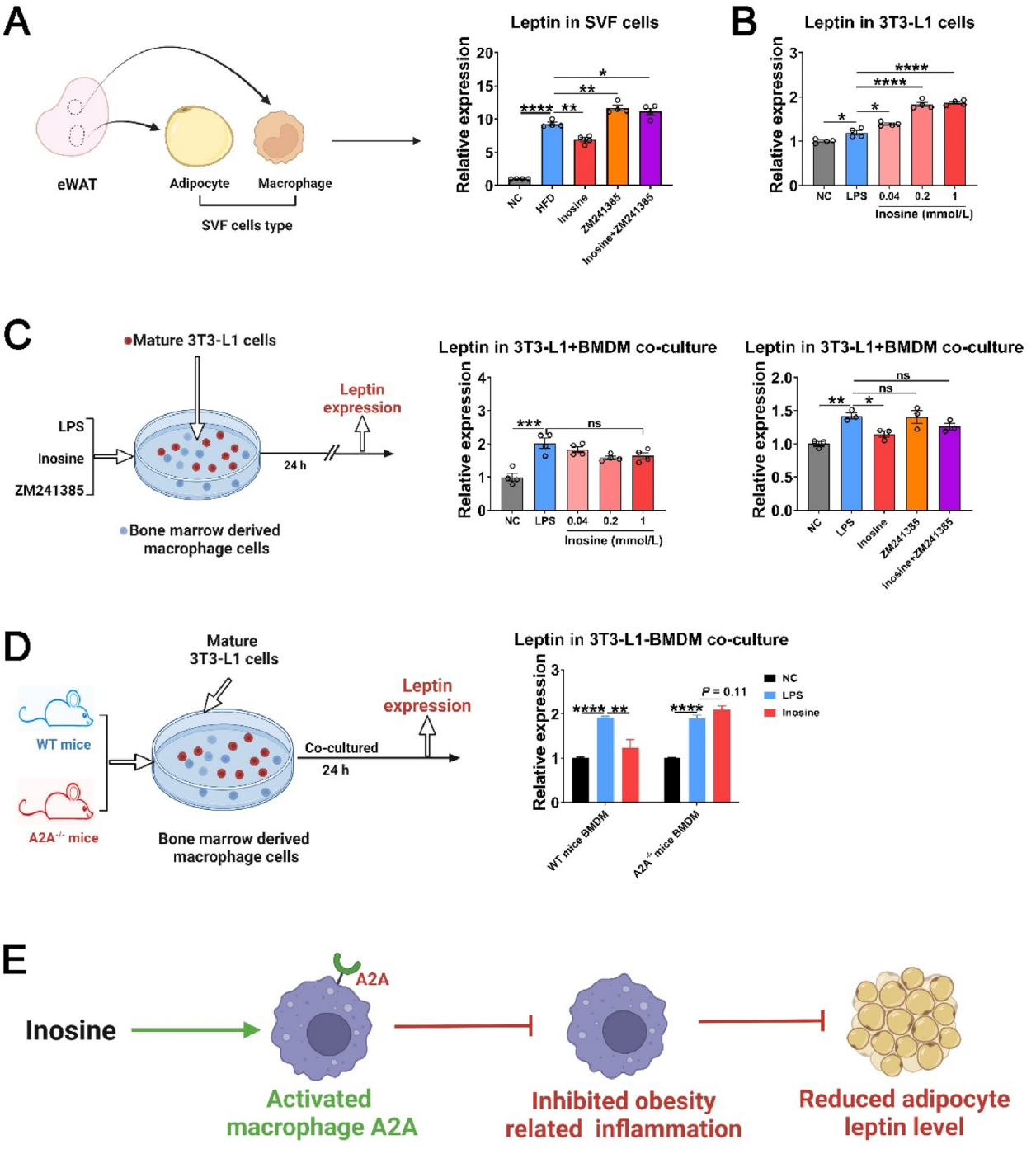

Figure 7 Inosine indirectly reduced adipocyte leptin levels by regulating macrophages. (A, B) Leptin expression levels in SVFs and 3T3-L1 cells ($n = 4$). (C, D) Leptin expression levels in BMDMs and 3T3-L1 cocultured cells ($n = 3$−4). (E) Inosine action flow. Data are shown as the mean ± SEM, $^{ns}P > 0.05$, $^{*}P < 0.05$, $^{**}P < 0.01$, $^{***}P < 0.001$, $^{****}P < 0.0001$ *versus* the other groups.

BMDMs with 3T3-L1 cells, and detecting leptin expression (Fig. 7C). The results showed that inosine inhibited leptin expression, and the inosine concentration had a certain positive correlation with leptin levels (Fig. 7C). In addition, the ability of inosine to reduce leptin expression levels in 3T3-L1 and BMDM cocultured cells treated with ZM241385 (Fig. 7C) or isolated from $A2A^{-/-}$ mice (Fig. 7D) was partially disrupted. In summary, inosine indirectly influenced adipocyte leptin secretion by regulating macrophage A2A signaling (Fig. 7E).

3.8. (Ex-4)$_2$-Fc partially reversed obesity-induced hypothalamic leptin resistance and improved obesity via A2A signaling

Finally, we used $A2A^{-/-}$ mice to verify whether (Ex-4)$_2$-Fc reversed obesity-induced hypothalamic leptin resistance *via* A2A signaling (Fig. 8A). We identified wild-type (WT) and $A2A^{-/-}$ mice by PCR (Supporting Information Fig. S6A). WT and $A2A^{-/-}$ mice were fed a high-fat diet to induce obesity (Fig. S6B−S6D). Compared to $A2A^{-/-}$ mice, WT mice showed more significant

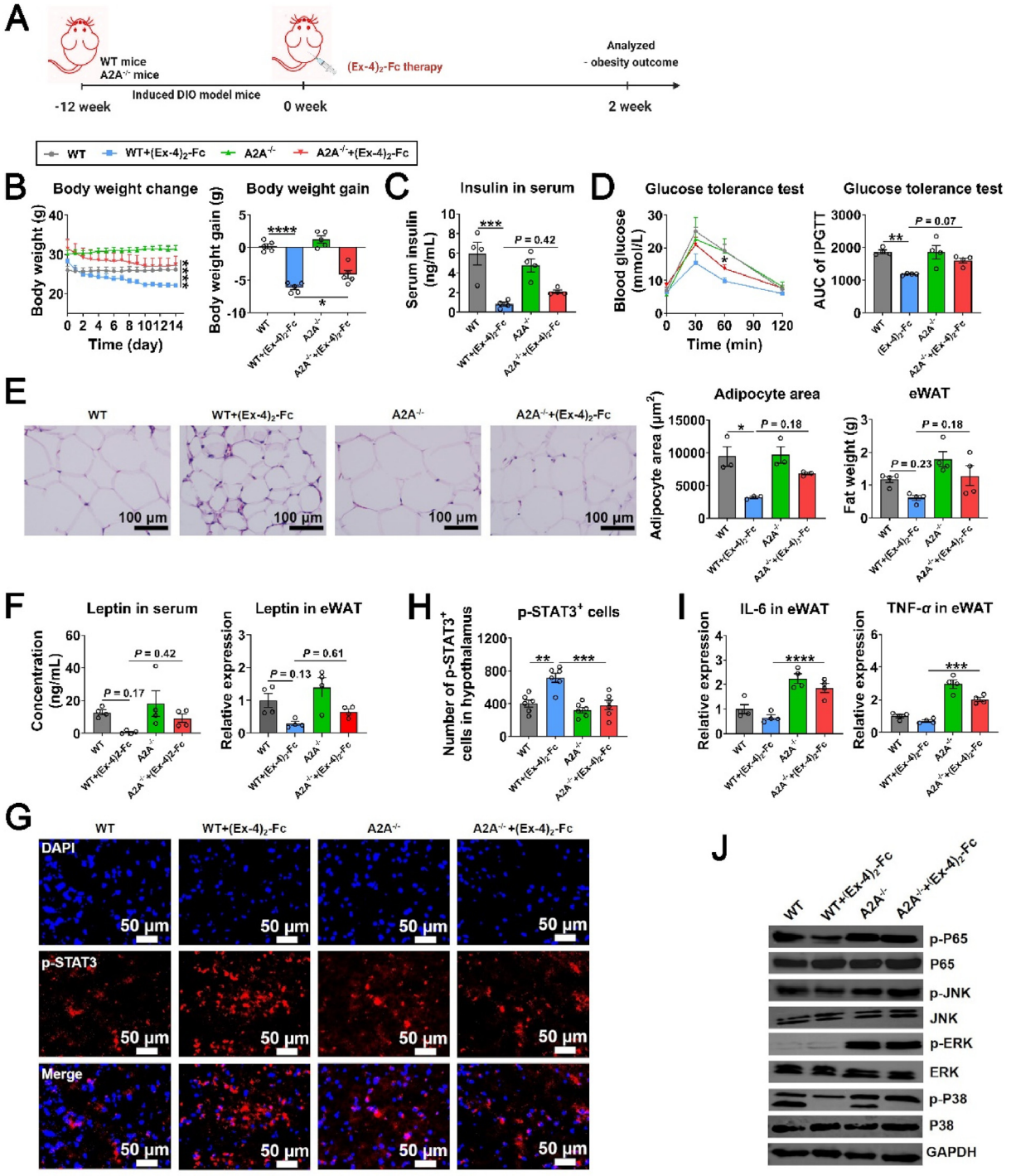

Figure 8 $(Ex\text{-}4)_2$-Fc partially reversed obesity-induced hypothalamic leptin resistance and improved obesity *via* A2A signaling. (A) Experimental schematic. (B) Body weight change ($n = 5$). (C) Insulin concentrations ($n = 4$). (D) Blood glucose levels ($n = 4$). (E) HE staining results and eWAT weight ($n = 3-4$). (F) Leptin levels ($n = 4$). (G, H) Immunofluorescence results and p-STAT3$^+$ cells in the hypothalamus ($n = 6$). (I) Proinflammatory factor expression ($n = 4$). (J) A2A pathway protein expression. Data are shown as the mean ± SEM, $^*P < 0.05$, $^{**}P < 0.01$, $^{***}P < 0.001$, $^{****}P < 0.0001$ *versus* the other groups.

weight loss and less body weight gain after $(Ex\text{-}4)_2$-Fc treatment (Fig. 8B), while food intake was greater (Fig. S2E). In addition, the improvement effect of $(Ex\text{-}4)_2$-Fc on insulin, glucose tolerance, and eWAT was also partially disrupted by the loss of A2A (Fig. 8C−E). The WT+$(Ex\text{-}4)_2$-Fc group showed lower leptin levels in serum and eWAT (Fig. 8F) and higher p-STAT3 expression in the hypothalamus (Fig. 8G and H). Similarly, the levels of relevant inflammatory markers in the WT $(Ex\text{-}4)_2$-Fc group were lower than those in the $A2A^{-/-}$ +$(Ex\text{-}4)_2$-Fc group (Fig. 8I and J, Supporting Information Fig. S7). Overall, these results show that

$(Ex\text{-}4)_2$-Fc partially reversed obesity-induced hypothalamic leptin resistance and improved obesity *via* A2A signaling.

4. Discussion

The gut microbiota was shown to make a crucial contribution to the development of obesity and metabolic disease[22-24]. Some studies have shown that GLP-1RAs, such as liraglutide, modulate the gut microbiota[41]. For example, liraglutide treatment in patients with T2D significantly increased the diversity and richness of the gut microbiota, particularly *Bacteroides*, *Proteobacteria*, and *Bacillus*[42]. In addition, it was also suggested that the reason why the use of GLP-1RAs had to be terminated in the trial due to GLP-1 resistance in clinical application may be related to gut microbiota imbalance[43,44]. In 2017, how gut microbiota dysbiosis induces GLP-1 resistance was well exhibited in mice[28]. In one human study, different groups of gut microbes were found to respond differently to GLP-1RAs[45]. Many studies have shown that GLP-1 is closely related to the functional gut microbiota[28,46,47]. Therefore, the characteristics of the gut microbiota can predict the efficacy of GLP-1RAs. However, a randomized controlled trial showed that liraglutide and sitagliptin did not change the alpha or beta diversity of the gut microbiota in adults with T2D[48]. In addition, a fixed combination of liraglutide and degludec for 6 months did not change the microbiome biodiversity or community among a group of very old T2D patients[49]. The possible reason was that the combination of drugs masked the effect[47]. Our research aimed to explore the mechanism of $(Ex\text{-}4)_2$-Fc from the perspective of the gut microbiota. We found that $(Ex\text{-}4)_2$-Fc induced a decrease in *Firmicutes* and *Proteobacteria* and an increase in *Bacteroidetes* and *Verrucomicrobia*. In particular, *Am* in *Verrucobacteria* increased significantly after $(Ex\text{-}4)_2$-Fc treatment. Similarly, some previous studies have also shown significant increases in intestinal *Am* abundance in wild-type obese mice and *db*/*db* mice treated with liraglutide[40,41,50,51]. However, the relationships between the gut microbiota, GLP-1, and the host are still unclear. At present, many studies on the correlation between GLP-1 and the gut microbiota are limited. In the future, the development of technologies will help explain and validate the relationship between GLP-1 and the gut microbiota. The clinical use of GLP-1RAs should consider the impact of the gut microbiota and should provide a personalized regimen.

To better elucidate the relationship between $(Ex\text{-}4)_2$-Fc treatment and the gut microbiota, previous studies have shown that the gut microbiota can interact with hosts through metabolites[41,52-55] and that drugs can also affect metabolism by changing the intestinal microflora and its metabolites[32]. Therefore, we explored the mechanism of $(Ex\text{-}4)_2$-Fc therapy through the gut microbiota or metabolites. The results confirmed that the therapeutic effect of $(Ex\text{-}4)_2$-Fc was partly related to the gut microbiota, and its therapeutic effect was related to *Am* and its metabolite inosine. In our previous studies, we found that $(Ex\text{-}4)_2$-Fc improved obesity and inhibited obesity-related inflammation by reducing leptin levels[10]. Leptin is a hormone secreted from adipocytes that acts on the hypothalamus to decrease food intake and increase energy expenditure, effects that require STAT3 signaling[32]. Studies have indicated that leptin signaling in the hypothalamus of obese mice not only remains functional but is also permanently activated[56]. This persistent activation was due to endogenous high circulating leptin concentrations, and there was a saturation of leptin signaling with a failure to further respond to even higher concentrations of exogenous leptin. Some recent reports indicated that partial leptin reduction in obese mice improved glucose tolerance and insulin sensitivity and reduced body weight[21,57], which is consistent with our current partial leptin reduction strategy. However, the potential mechanism of action of GLP-1RAs in the treatment of obesity through the leptin pathway has not been understood until now. Based on the finding that $(Ex\text{-}4)_2$-Fc treatment can increase inosine and reverse obesity-induced hypothalamic leptin antagonism, we hypothesized that it may regulate body leptin levels through the metabolite inosine. Indeed, we found that inosine therapy reversed obesity-induced hypothalamic leptin antagonism and ameliorated obesity through the leptin pathway in *db*/*db* and *ob*/*ob* mice. Moreover, studies have demonstrated that inosine mediates proinflammatory cytokine production, which is partially reversed by the A2A antagonist DMPX[38]. Similarly, our study revealed that the reduction in proinflammatory cytokine production induced by inosine was partially reversed by ZM241385. Moreover, inosine decreased adipocyte leptin levels indirectly by regulating macrophage A2A. In addition, inosine-mediated improvements in obesity were partly dependent on the A2A pathway (Supporting Information Fig. S8). We further verified that $(Ex\text{-}4)_2$-Fc reversed leptin antagonism through A2A signaling in $A2A^{-/-}$ mice.

5. Conclusions

Our study revealed that GLP-1RAs partially reversed obesity-induced hypothalamic leptin antagonism through microbiota-driven inosine and provided new insights into guiding the clinical use of antidiabetic agents.

Acknowledgments

This study was supported by the 1.3.5 Project for Disciplines of Excellence (No. ZYGD18007), West China Hospital, Sichuan University, the Natural Science Foundation Project of Sichuan Province (No. 2022NSFSC1309, China) and the National Natural Science Foundation of China (No. 82203016). The authors would like to thank Dr. Zhou and Dr. Zhao for their help with gut microbiota and metabolic analysis. The authors also like to acknowledge Dr. Zhang, Dr. Tian, Dr. Xie, and Dr. Wu for their assistance with the collection of relevant experimental samples. The authors thank Lin for her help in the animal experiments. Prof. Li Yang is the guarantor of this work; as such, she has full access to all the data in the study and is responsible for the integrity of the data and the accuracy of the data analysis.

Author contributions

Chunyan Dong: Writing − original draft. Bailing Zhou: Methodology, Formal analysis. Binyan Zhao: Methodology. Ke Lin: Investigation. Yaomei Tian: Investigation. Rui Zhang: Resources. Daoyuan Xie: Resources. Siwen Wu: Resources, Methodology. Li Yang: Writing − review & editing, Project administration, Data curation, Conceptualization.

Conflicts of interest

The authors declare no conflicts of interest.

Appendix A. Supplementary information

Supporting information to this article can be found online at https://doi.org/10.1016/j.apsb.2024.12.006.

References

1. Ortega MA, Fraile-Martínez O, Naya I, García-Honduvilla N, Álvarez-Mon M, Buján J, et al. Type 2 Diabetes mellitus associated with obesity (diabesity). The central role of gut microbiota and its translational applications. *Nutrients* 2020;**12**:2749.
2. Sebag SC, Hao M, Qian Q, Upara C, Ding Q, Zhu M, et al. A medium chain fatty acid, 6-hydroxyhexanoic acid (6-HHA), protects against obesity and insulin resistance. *Acta Pharm Sin B* 2024;**14**:1892−4.
3. Xu Z, Liu D, Liu D, Ren X, Liu H, Qi G, et al. Equisetin is an anti-obesity candidate through targeting 11β-HSD1. *Acta Pharm Sin B* 2022;**12**:2358−73.
4. Ding L, Yang Q, Zhang E, Wang Y, Sun S, Yang Y, et al. Notoginsenoside Ft1 acts as a TGR5 agonist but FXR antagonist to alleviate high fat diet-induced obesity and insulin resistance in mice. *Acta Pharm Sin B* 2021;**11**:1541−54.
5. Graaf C, Donnelly D, Wootten D, Lau J, Sexton PM, Miller LJ, et al. Glucagon-like peptide-1 and its class B G protein-coupled receptors: a long march to therapeutic successes. *Pharmacol Rev* 2016;**68**:954−1013.
6. Murage EN, Gao G, Bisello A, Ahn JM. Development of potent glucagon-like peptide-1 agonists with high enzyme stability *via* introduction of multiple lactam bridges. *J Med Chem* 2010;**53**:6412−20.
7. Baggio LL, Drucker DJ. Biology of incretins: GLP-1 and GIP. *Gastroenterology* 2007;**132**:2131−57.
8. Thorens B, Porret A, Bühler L, Deng SP, Morel P, Widmann C. Cloning and functional expression of the human islet GLP-1 receptor. Demonstration that exendin-4 is an agonist and exendin-(9−39) an antagonist of the receptor. *Diabetes* 1993;**42**:1678−82.
9. Davies M, Heller S, Sreenan S, Sapin H, Adetunji O, Tahbaz A, et al. Once-weekly exenatide versus once- or twice-daily insulin detemir: randomized, open-label, clinical trial of efficacy and safety in patients with type 2 diabetes treated with metformin alone or in combination with sulfonylureas. *Diabetes Care* 2013;**36**:1368−76.
10. Zhou B, Dong C, Zhao B, Su X, Luo Y, Xie L, et al. (E_X-4)2-Fc, an effective long-acting GLP-1 receptor agonist, reduces obesity-related inflammation by inhibiting leptin expression. *Biochem Biophys Res Commun* 2020;**529**:562−8.
11. Lu L, Su X, Wang Y, Luo Y, Yang J, Xie L, et al. *In vitro* and *in vivo* characterization of a novel long-acting GLP-1 receptor agonist, exendin-4−Fc fusion protein. *RSC Adv* 2017;**7**:54178−87.
12. Apovian CM, Aronne LJ, Bessesen DH, McDonnell ME, Murad MH, Pagotto U, et al. Pharmacological management of obesity: an Endocrine Society clinical practice guideline. *J Clin Endocrinol Metab* 2015;**100**:342−62.
13. Wilding JPH, Batterham RL, Calanna S, Davies M, Van Gaal LF, Lingvay I, et al. Once-weekly semaglutide in adults with overweight or obesity. *N Engl J Med* 2021;**384**:989−1002.
14. O'Neil PM, Birkenfeld AL, McGowan B, Mosenzon O, Pedersen SD, Wharton S, et al. Efficacy and safety of semaglutide compared with liraglutide and placebo for weight loss in patients with obesity: a randomised, double-blind, placebo and active controlled, dose-ranging, phase 2 trial. *Lancet* 2018;**392**:637−49.
15. Ghusn W, De la Rosa A, Sacoto D, Cifuentes L, Campos A, Feris F, et al. Weight loss outcomes associated with semaglutide treatment for patients with overweight or obesity. *JAMA Netw Open* 2022;**5**:e2231982.
16. Garvey WT, Batterham RL, Bhatta M, Buscemi S, Christensen LN, Frias JP, et al. Two-year effects of semaglutide in adults with overweight or obesity: the STEP 5 trial. *Nat Med* 2022;**28**:2083−91.
17. Kjems LL, Holst JJ, Vølund A, Madsbad S. The influence of GLP-1 on glucose-stimulated insulin secretion: effects on beta-cell sensitivity in type 2 and nondiabetic subjects. *Diabetes* 2003;**52**:380−6.
18. Campbell JE, Drucker DJ. Pharmacology, physiology, and mechanisms of incretin hormone action. *Cell Metab* 2013;**17**:819−37.
19. Drucker DJ, Nauck MA. The incretin system: glucagon-like peptide-1 receptor agonists and dipeptidyl peptidase-4 inhibitors in type 2 diabetes. *Lancet* 2006;**368**:1696−705.
20. Gallwitz B. Glucagon-like peptide-1 analogues for Type 2 diabetes mellitus: current and emerging agents. *Drugs* 2011;**71**:1675−88.
21. Zhao S, Zhu Y, Schultz RD, Li N, He Z, Zhang Z, et al. Partial leptin reduction as an insulin sensitization and weight loss strategy. *Cell Metab* 2019;**30**:706−19.e6.
22. Qin J, Li Y, Cai Z, Li S, Zhu J, Zhang F, et al. A metagenome-wide association study of gut microbiota in type 2 diabetes. *Nature* 2012;**490**:55−60.
23. Wrzosek L, Ciocan D, Hugot C, Spatz M, Dupeux M, Houron C, et al. Microbiota tryptophan metabolism induces aryl hydrocarbon receptor activation and improves alcohol-induced liver injury. *Gut* 2021;**70**:1299−308.
24. Yasir M, Angelakis E, Bibi F, Azhar EI, Bachar D, Lagier JC, et al. Comparison of the gut microbiota of people in France and Saudi Arabia. *Nutr Diabetes* 2015;**5**:e153.
25. Sun L, Pang Y, Wang X, Wu Q, Liu H, Liu B, et al. Ablation of gut microbiota alleviates obesity-induced hepatic steatosis and glucose intolerance by modulating bile acid metabolism in hamsters. *Acta Pharm Sin B* 2019;**9**:702−10.
26. Knop FK, Aaboe K, Vilsbøll T, Vølund A, Holst JJ, Krarup T, et al. Impaired incretin effect and fasting hyperglucagonaemia characterizing type 2 diabetic subjects are early signs of dysmetabolism in obesity. *Diabetes Obes Metab* 2012;**14**:500−10.
27. Muscelli E, Mari A, Casolaro A, Camastra S, Seghieri G, Gastaldelli A, et al. Separate impact of obesity and glucose tolerance on the incretin effect in normal subjects and type 2 diabetic patients. *Diabetes* 2008;**57**:1340−8.
28. Grasset E, Puel A, Charpentier J, Collet X, Christensen JE, Tercé F, et al. A specific gut microbiota dysbiosis of type 2 diabetic mice induces GLP-1 resistance through an enteric NO-dependent and gut−brain axis mechanism. *Cell Metab* 2017;**25**:1075−90.e5.
29. Andoh A, Nishida A, Takahashi K, Inatomi O, Imaeda H, Bamba S, et al. Comparison of the gut microbial community between obese and lean peoples using 16S gene sequencing in a Japanese population. *J Clin Biochem Nutr* 2016;**59**:65−70.
30. Gao X, Zhang M, Xue J, Huang J, Zhuang R, Zhou X, et al. Body mass index differences in the gut microbiota are gender specific. *Front Microbiol* 2018;**9**:1250.
31. Routy B, Le Chatelier E, Derosa L, Duong CPM, Alou MT, Daillère R, et al. Gut microbiome influences efficacy of PD-1-based immunotherapy against epithelial tumors. *Science* 2018;**359**:91−7.
32. Whang A, Nagpal R, Yadav H. Bi-directional drug-microbiome interactions of anti-diabetics. *EBioMedicine* 2019;**39**:591−602.
33. Mager LF, Burkhard R, Pett N, Cooke NCA, Brown K, Ramay H, et al. Microbiome-derived inosine modulates response to checkpoint inhibitor immunotherapy. *Science* 2020;**369**:1481−9.
34. Vétizou M, Pitt JM, Daillère R, Lepage P, Waldschmitt N, Flament C, et al. Anticancer immunotherapy by CTLA-4 blockade relies on the gut microbiota. *Science* 2015;**350**:1079−84.
35. Sivan A, Corrales L, Hubert N, Williams JB, Aquino-Michaels K, Earley ZM, et al. Commensal bifidobacterium promotes antitumor immunity and facilitates anti-PD-L1 efficacy. *Science* 2015;**350**:1084−9.
36. Yu AM, Ingelman-Sundberg M, Cherrington NJ, Aleksunes LM, Zanger UM, Xie W, et al. Regulation of drug metabolism and toxicity by multiple factors of genetics, epigenetics, lncRNAs, gut microbiota, and diseases: a meeting report of the 21st International Symposium on Microsomes and Drug Oxidations (MDO). *Acta Pharm Sin B* 2017;**7**:241−8.
37. Zhang X, Han Y, Huang W, Jin M, Gao Z. The influence of the gut microbiota on the bioavailability of oral drugs. *Acta Pharm Sin B* 2021;**11**:1789−812.
38. Welihinda AA, Kaur M, Greene K, Zhai Y, Amento EP. The adenosine metabolite inosine is a functional agonist of the adenosine A2A receptor with a unique signaling bias. *Cell Signal* 2016;**28**:552−60.
39. Köröskényi K, Kiss B, Szondy Z. Adenosine A2A receptor signaling attenuates LPS-induced pro-inflammatory cytokine formation of mouse macrophages by inducing the expression of DUSP1. *Biochim Biophys Acta* 2016;**1863**:1461−71.

40. Pei Y, Li H, Cai Y, Zhou J, Luo X, Ma L, et al. Regulation of adipose tissue inflammation by adenosine 2A receptor in obese mice. *J Endocrinol* 2018;**239**:365−76.
41. Moreira GV, Azevedo FF, Ribeiro LM, Santos A, Guadagnini D, Gama P, et al. Liraglutide modulates gut microbiota and reduces NAFLD in obese mice. *J Nutr Biochem* 2018;**62**:143−54.
42. Ying X, Rongjiong Z, Kahaer M, Chunhui J, Wulasihan M. Therapeutic efficacy of liraglutide *versus* metformin in modulating the gut microbiota for treating type 2 diabetes mellitus complicated with nonalcoholic fatty liver disease. *Front Microbiol* 2023;**14**:1088187.
43. Hemmer A, Maiter D, Buysschaert M, Preumont V. Long-term effects of GLP-1 receptor agonists in type 2 diabetic patients: a retrospective real-life study in 131 patients. *Diabetes Metab Syndr* 2019;**13**:332−6.
44. Gill SR, Pop M, Deboy RT, Eckburg PB, Turnbaugh PJ, Samuel BS, et al. Metagenomic analysis of the human distal gut microbiome. *Science* 2006;**312**:1355−9.
45. Tsai CY, Lu HC, Chou YH, Liu PY, Chen HY, Huang MC, et al. Gut microbial signatures for glycemic responses of GLP-1 receptor agonists in type 2 diabetic patients: a pilot study. *Front Endocrinol* 2021;**12**:814770.
46. Zhang X, Ren H, Zhao C, Shi Z, Qiu L, Yang F, et al. Metagenomic analysis reveals crosstalk between gut microbiota and glucose-lowering drugs targeting the gastrointestinal tract in Chinese patients with type 2 diabetes: a 6 month, two-arm randomised trial. *Diabetologia* 2022;**65**:1613−26.
47. Zeng Y, Wu Y, Zhang Q, Xiao X. Crosstalk between glucagon-like peptide 1 and gut microbiota in metabolic diseases. *mBio* 2024;**15**:e0203223.
48. Smits MM, Fluitman KS, Herrema H, Davids M, Kramer MHH, Groen AK, et al. Liraglutide and sitagliptin have no effect on intestinal microbiota composition: a 12-week randomized placebo-controlled trial in adults with type 2 diabetes. *Diabetes Metab* 2021;**47**:101223.
49. Rizza S, Pietrucci D, Longo S, Menghini R, Teofani A, Piciucchi G, et al. Impact of insulin degludec/liraglutide fixed combination on the gut microbiomes of elderly patients with type 2 diabetes: results from a subanalysis of a small non-randomised single arm study. *Aging Dis* 2023;**14**:319−24.
50. Liu Q, Cai BY, Zhu LX, Xin X, Wang X, An ZM, et al. Liraglutide modulates gut microbiome and attenuates nonalcoholic fatty liver in *db/db* mice. *Life Sci* 2020;**261**:118457.
51. Wang H, Wang L, Li Y, Luo S, Ye J, Lu Z, et al. The HIF-2α/PPARα pathway is essential for liraglutide-alleviated, lipid-induced hepatic steatosis. *Biomed Pharmacother* 2021;**140**:111778.
52. Postler TS, Ghosh S. Understanding the holobiont: how microbial metabolites affect human health and shape the immune system. *Cell Metab* 2017;**26**:110−30.
53. Chen P, Torralba M, Tan J, Embree M, Zengler K, Stärkel P, et al. Supplementation of saturated long-chain fatty acids maintains intestinal eubiosis and reduces ethanol-induced liver injury in mice. *Gastroenterology* 2015;**148**:203−14.e16.
54. Hartmann P, Hochrath K, Horvath A, Chen P, Seebauer CT, Llorente C, et al. Modulation of the intestinal bile acid/farnesoid X receptor/fibroblast growth factor 15 axis improves alcoholic liver disease in mice. *Hepatology* 2018;**67**:2150−66.
55. Hendrikx T, Duan Y, Wang Y, Oh JH, Alexander LM, Huang W, et al. Bacteria engineered to produce IL-22 in intestine induce expression of REG3G to reduce ethanol-induced liver disease in mice. *Gut* 2019;**68**:1504−15.
56. Balland E, Chen W, Tiganis T, Cowley MA. Persistent leptin signaling in the arcuate nucleus impairs hypothalamic insulin signaling and glucose homeostasis in obese mice. *Neuroendocrinology* 2019;**109**:374−90.
57. Balland E, Chen W, Dodd GT, Conductier G, Coppari R, Tiganis T, et al. Leptin signaling in the arcuate nucleus reduces insulin's capacity to suppress hepatic glucose production in obese mice. *Cell Rep* 2019;**26**:346−55.e3.